Physics Letters A 381 (2017) 3845–3848

Contents lists available at ScienceDirect

Physics Letters A

www.elsevier.com/locate/pla

Hermite scatterers in an ultraviolet sky

Kevin J. Parker

Department of Electrical and Computer Engineering, University of Rochester, Hopeman Building 203, Box 270126, Rochester, NY 14627, USA

ARTICLE INFO

Article history:
Received 10 August 2017
Received in revised form 10 October 2017
Accepted 12 October 2017
Available online 16 October 2017
Communicated by M.G.A. Paris

Keywords:
Scattering
Rayleigh scattering
Electromagnetics
Optics
Acoustics
Hermite polynomials

ABSTRACT

The scattering from spherical inhomogeneities has been a major historical topic in acoustics, optics, and electromagnetics and the phenomenon shapes our perception of the world including the blue sky. The long wavelength limit of "Rayleigh scattering" is characterized by intensity proportional to k^4 (or λ^{-4}) where k is the wavenumber and λ is the wavelength. With the advance of nanotechnology, it is possible to produce scatterers that are inhomogeneous with material properties that are functions of radius r, such as concentric shells. We demonstrate that with proper choice of material properties linked to the Hermite polynomials in r, scatterers can have long wavelength scattering behavior of higher powers: k^8, k^{16}, and higher. These "Hermite scatterers" could be useful in providing unique signatures (or colors) to regions where they are present. If suspended in air under white light, the back-scattered spectrum would be shifted from blue towards violet and then ultraviolet as the higher order Hermite scatterers were illuminated.

1. Introduction

The scattering of acoustic and electromagnetic waves from inhomogeneities has a long history [18,16]. The long wavelength or Rayleigh scattering regime is present in daily phenomena, from the blue sky to the scattering of ultrasound by blood in Doppler studies of vasculature. We show that a class of inhomogeneous scatterers called Hermite scatterers of odd integer order m can produce a long wavelength scattering amplitude proportional to wavenumber k^{m+1}, that is: k^2, k^4, k^6, and so forth. The result is significant since advances in nanotechnology are enabling the manufacture of tailored concentric "onion layer" spherical particles of different materials [2,15], and Hermite scatterers of order m can be detected and classified by their unique power law signatures. This paper reviews some central relationships for simple acoustic and then electromagnetic scattering, identifying a common integral kernel. Then, the scattering inhomogeneities are represented by modified Hermite orders to produce higher power law scattering, with examples.

2. Theory

2.1. Scattering of acoustic waves

In this section, we examine the backscattered pressure from an inhomogeneity of compressibility, following the classical approach described in Chapter 8 of Morse and Ingard [11]. This treatment begins under the Born approximation (weak scatterers) with an incident plane wave P_i of frequency ω traveling in the x-direction:

$$P_i = A\mathbf{e}^{ikx}, \tag{1}$$

where A is the amplitude, $k = \omega/c$ is the wavenumber, c is the speed of sound, and the $\mathbf{e}^{-i\omega t}$ term is implicit throughout. Then, the backscattered pressure P_{bs} is approximately

$$P_{bs}(k, x) \cong A\left(\frac{\mathbf{e}^{ikx}}{x}\right)\left(\frac{k^2}{4\pi}\right)\iiint \kappa(r)\,\mathbf{e}^{i2\hat{\boldsymbol{k}}\bullet\hat{\mathbf{r}}}dVol, \tag{2}$$

where $\kappa(r)$ is the (small) fractional change in compressibility within the scatterer, assumed to vary only in the radial dimension, the $2\hat{k}$ term in the complex exponential comes from the 180° direction of backscatter, and the integration is over the scattering volume. This equation has the form of a spatial Fourier transform of the scatterer. Next we assume an isotropic spherical $\kappa(r)$, and utilize spherical coordinates where the polar angle θ is aligned with the x-axis coordinate system, and $\hat{\boldsymbol{k}}$ is oriented along the x-axis. Then $\hat{\boldsymbol{k}} \cdot \hat{\mathbf{r}} = kr\cos\theta$, $dVol = r^2 \sin\theta d\theta d\phi$, and the volume integral becomes

$$\begin{aligned} VI_1(k) &= \iiint \kappa(r)\,\mathbf{e}^{i2\hat{\boldsymbol{k}}\bullet\hat{\mathbf{r}}}dVol \\ &= \int_{r=0}^{\infty}\int_{\theta=0}^{\pi}\int_{\phi=0}^{2\pi} \kappa(r)\,\mathbf{e}^{i2kr\cos\theta} r^2 \sin\theta d\theta d\phi. \end{aligned} \tag{3}$$

E-mail address: kevin.parker@rochester.edu.

https://doi.org/10.1016/j.physleta.2017.10.019
0375-9601/

Integrating first over ϕ then θ yields

$$V I_1 (k) = \left(\frac{2\pi}{k}\right) \int_{r=0}^{\infty} r \cdot \kappa (r) \cdot \sin (2kr)\, dr. \tag{4}$$

For the classical solution, we assume a uniform sphere of $\kappa (r) = \kappa_0\, (0 \le r \le a)$ and zero elsewhere, then eqn (4) becomes

$$V I_1 (k) = \kappa_0 4\pi a^3 \left(\frac{j_1 (2ka)}{2ka}\right). \tag{5}$$

Thus, from eqn (2),

$$P_{bs} (k, x) \cong A_1 \kappa_0 \left(\frac{\mathbf{e}^{ikx}}{x}\right) \left(k^2\right) \left(a^3\right) \left(\frac{j_1 (2ka)}{2ka}\right). \tag{6}$$

In the long wavelength limit as $ka \to 0$, the $j_1 (2ka) / 2ka$ term approaches a constant $(= 1/3)$, and we have the classical Rayleigh scattering proportional to k^2 and a^3 as shown in eqn 8.1.21 of Morse and Ingard [11]. When considering scattering from random media, it can be shown [8,9,4] that formulas similar to eqn (2)–(4) apply to relationships between the differential scattering cross section per unit volume $\sigma_d (k)$ and the spatial correlation $b (\hat{r})$ function of the inhomogeneities such that

$$\sigma_d (k) = k^4 A \iiint b (\hat{r})\, \mathbf{e}^{j2\hat{k}\cdot\hat{r}} dVol, \tag{7}$$

and assuming the correlation function is isotropic and simply dependent on distance r, the volume integral reduces to

$$V I_2 (k) = \int_0^{\infty} r \cdot b (r) \sin (2kr)\, dr, \tag{8}$$

similar to the integral found in eqn (4) for the single inhomogeneity. A derivation resulting in the $j_1 (2ka) / 2ka$ form factor is also well established for ensemble-averaged differential cross-section backscatter coefficients for randomly positional spheres in a medium [8,9].

2.2. Scattering of electromagnetic waves

Early treatments of light scattering from conducting spheres include works by Garnett [7] and Mie [10]. In classical solutions, the scattered wave is composed of a series of spherical harmonics of ascending orders [3]. In the long wavelength limit only the first partial wave is considered and the solution reduces to the familiar Rayleigh scattering behavior, amplitude proportional to k^2 (or inversely proportional to $1/\lambda^2$) and intensity proportional to k^4 or $1/\lambda^4$.

In 1918, Lord Rayleigh formulated the equations for scattering from a spherical weak inhomogeneity, applying a differential approach considering an infinitesimally thin shell of small change in index [17]. The differential approach leads directly to integral formulations across inhomogeneous spheres resembling the integral equations from acoustics in the previous section. From Rayleigh's eqn (3), (6) and (7), and examining the backscatter (angle $\chi = 0$ in his notation for which $m = 2kr \cos \left(\frac{1}{2}\chi\right) = 2kr$ in the case of backscatter) we can write for a sphere of radius a:

$$\begin{aligned} \phi_R (k) &\cong \frac{k^2}{4\pi} \left(\frac{\mathbf{e}^{-ikx}}{x}\right) \int_0^{a} \gamma (r) \left(4\pi r^2\right) \left(\frac{\sin (2kr)}{(2kr)}\right) dr \\ &= \frac{k}{2} \left(\frac{\mathbf{e}^{-ikx}}{x}\right) \int_0^{a} r \cdot \gamma (r) \cdot \sin (2kr)\, dr, \end{aligned} \tag{9}$$

where $\gamma (r)$ is the small change in index of refraction (the quantity $\mathrm{K} - 1$ in Rayleigh's notation) and $\phi_R (k)$ is "the electric displacements in the scattered wave, so far as they depend upon the first power of $\mathrm{K}-1\ldots$ at a great distance." For the homogeneous sphere of $\gamma_0 (r) = \gamma_0$ and radius a, Rayleigh's integral produces his eqn (5), which for backscatter angle $\chi = 0$ and using our notation becomes:

$$\begin{aligned} \phi_R (k) &= \gamma_0 \left(\frac{\mathbf{e}^{-ikx}}{x}\right) k^2 a^3 \left(\frac{\sin 2ka}{(2ka)^3} - \frac{\cos 2ka}{(2ka)^2}\right) \\ &= \gamma_0 \left(\frac{\mathbf{e}^{-ikx}}{x}\right) k^2 a^3 \left(\frac{j_i (2ka)}{(2ka)}\right), \end{aligned} \tag{10}$$

using the expansion identity of the spherical Bessel function. We note this is equivalent to our eqn (6) for the scattering of a sphere in acoustics.

A statistical approach to scattering from small fluctuations in dielectric constant characterized by the spatial correlation function $\hat{\gamma} (r)$ was later introduced by Debye and Bueche [5]. For isotropic $\hat{\gamma} (r)$ and for the backscatter angle, their eqn ($3''$) reduces to

$$\left|\phi_s (k)\right|^2 \sim \left(\frac{2\pi}{k}\right) \bar{\eta}^2 V \int_0^{\infty} r \cdot \hat{\gamma} (r) \cdot \sin (2kr)\, dr, \tag{11}$$

where $\left|\phi_s (k)^2\right|$ is the backscattered intensity, $\bar{\eta}^2$ is the root mean square variation in dielectric constant around its mean value in the medium, and V is the illuminated volume. The integrand in eqn (11) is similar to that following eqn (8) for acoustic inhomogeneities, and eqn (9) for the case of electromagnetic waves, and also resembles eqn (4). The similarity of the integrands allows for common conclusions about special forms for $\kappa (r)$, $b (r)$, $\gamma (r)$, and $\hat{\gamma} (r)$.

2.3. New Hermite scatterers

Rewriting eqn (2)–(4) for the case of an inhomogeneous $\kappa (r)$, let us define

$$\phi_s (k) = \frac{k}{2} \int_0^{\infty} r \cdot \kappa (r) \cdot \sin (2kr)\, dr. \tag{12}$$

Now, let

$$\kappa_m (r) = \frac{\mathbf{G}H_m (r/R)}{r} \tag{13}$$

designate a "Hermite scatterer," where $m \in$ odd integer ≥ 1; R is a reference radius or scale factor, $\mathbf{G}H_m (r/R) = \mathbf{e}^{-(r/R)^2} H_m (r/R)$, and H_m is the mth order Hermite polynomial formed through the mth differentiation of a Gaussian function [1,14]. The odd orders are chosen as they approach zero as $r \to 0$, however the quotient $\mathbf{G}H_m (r/R) / r$ reaches a finite maximum at $r = 0$. Examples of these are shown in Fig. 1, where $m = 3, 5,$ and 7.

Substituting the Hermite $\kappa_m (r)$ into eqn (12):

$$\begin{aligned} \phi_s (k) &= \frac{k}{2} \int_0^{\infty} \mathbf{G}H_m (r/R) \sin (2kr)\, dr \\ &= -\sqrt{\pi} 2^{(m-2)} \cdot \mathbf{e}^{-(kR)^2} \cdot \left(-k^2 R^2\right)^{\frac{m+1}{2}}. \end{aligned} \tag{14}$$

For example, if $\kappa_m (r/R) = \kappa_7 (r/R) = \mathbf{G}H_7 (r/R)/r$, then $\phi_s (k)|_{m=7} = -\sqrt{\pi} 32 \mathbf{e}^{-(kR)^2} (kR)^8$. Note the general relation for long wavelengths where $(kR) \ll 1$ is $\phi_s (k)|_m \approx k^{m+1}$, which reduces to

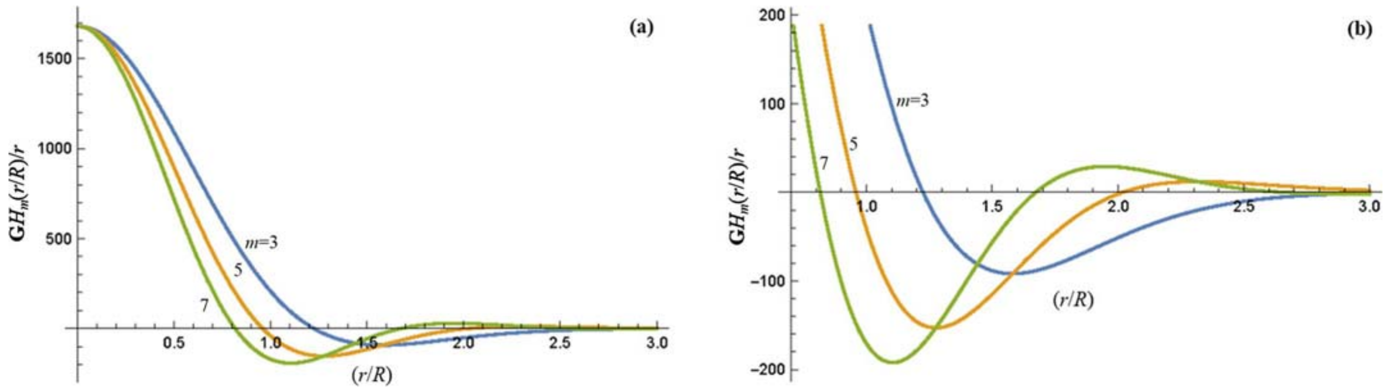

Fig. 1. (a) Modified Hermite functions $\mathbf{G}H_m(r/R)/r$ (arbitrary units) for $m = 3, 5, 7$ representing odd integer orders. This function provides the recipe for spherical scatterer properties as a function of radius, expressed as fractional change from the baseline properties of the surrounding medium. (b) Close-up of the modified Hermite scattering functions near their zero crossings. In physical terms, negative values correspond to acoustic or electromagnetic material properties slightly less than those of the surrounding medium.

Rayleigh scattering for $m = 1$ (k^2 dependence), but can be arbitrarily high depending on the ability to create stable concentric (continuous) spherical gradients in the form of $\kappa_m(r) = \mathbf{G}H_m(r/R)/r$.

3. Discussion

Lord Rayleigh's analysis of scattering from a differential shell element allowed him to also formulate the case of periodic fluctuations of inhomogeneities $\gamma(\hat{r})$ within a sphere [17], and this produced a scattering formula that was strongly angle-dependent. He speculated that "a structure of this sort is the cause of the remarkable colours, variable with the angle of observation, which are so frequent in beetles, butterflies, and feathers." Thus, the idea that special $\gamma(r)$ patterns produce distinct scattering effects is at least 100 years old. However, this understanding has been conditioned by the familiar long-wavelength behavior as k^2 (or k^4 in intensity) that has been seen repeatedly over many situations in optics, electromagnetics, and acoustics. Because of this established familiarity, it must be emphasized that the Rayleigh scattering power laws are *not* the upper limit on long wavelength scattering. There is, in theory, a formulation of average differential backscatter using a modified Gaussian autocorrelation function with zero mean, proposed in [11] (see chapter 8) and more fully developed by Waag et al. [20] (see his eqn (11) and (12)), and also in Waag et al. [19]. This function produces a long wavelength limit that includes a higher power law dependence on radius and frequency than the classical Rayleigh result. In fact, Waag has reported average differential scattering cross section per unit volume measurements with frequency dependences nearing frequency to the fifth power in certain scattering phantoms (see Figure 6 of [4]), and note that these results are measured in terms of ensemble averages and intensity variables (pressure squared). Thus, Waag proved that it is possible that for a subset of scatterers, a frequency dependence of higher than k^4 for intensity (k^2 for amplitude) is possible.

One way of assessing all of these results is by considering the common volume integral $\int_0^a r \cdot f(r) \cdot \sin(2kr)\, dr$ as the Fourier sine transform of $r \cdot f(r)$, where $f(r)$ represents the spatial spherical inhomogeneity. In this view, the Fourier transform of the modified Gaussian functions proposed by Morse and Ingard [11] and Waag et al. [19] are seen to have a sharp decrease to zero transform frequency (representing the long-wavelength limit). In a similar vein, the $\mathbf{G}H_m$ functions have leading power law terms in their Fourier sine transforms [14]. Thus, the negative sidelobes seen in Fig. 1 are essential for decreasing to zero the low frequency part of the Fourier sine transform, and under a precise power law. Furthermore, this interpretation suggests that any of the realizable functions shown in tables of Fourier sine transforms – for example, Erdélyi and Batemen [6] – will yield particular scattering solutions if implemented as a spherical inhomogeneity.

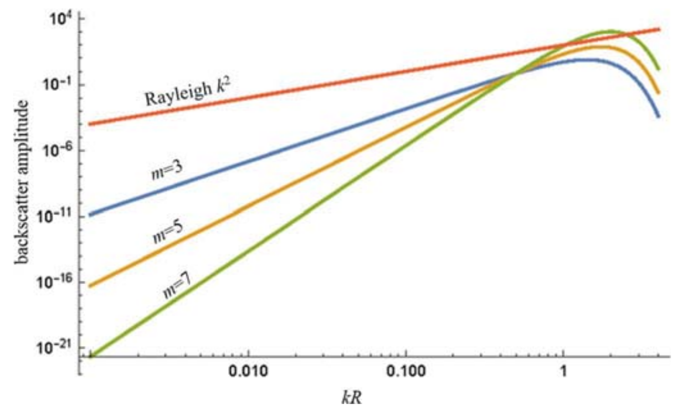

Fig. 2. Backscatter amplitude (arbitrary units) vs. normalized wavenumber kR -on a log–log scale. From upper to lower are shown the Rayleigh scattering k^2 regime, then results from Hermite scatterers of orders 3, 5, and 7. These illustrate the increasing power laws associated with higher order Hermite scatterers.

The long-wavelength scattering regime is also important in the H-scan classification of scatterers since the k^2 (or ω^2) frequency transfer function will convert a $\mathbf{G}H4$ pulse to a $\mathbf{G}H6$ echo [12, 13]. With Hermite scatterers present, a transmitted $\mathbf{G}H_n$ pulse will be backscattered as a $\mathbf{G}H_{(n+m+1)}$ pulse, and this enables advanced classification and identification schemes.

Finally, we note that the k^{m+1} long wavelength backscatter is valid to approximately $kR = 1$, as shown in Fig. 2. For example, if Hermite scatterers are constructed for visible light up to ultraviolet (UVA) at $\lambda = 400$ nm, then $kR = 1$ when the reference radius $R = \lambda/2\pi \approx 64$ nm. However, the Hermite $\kappa(r)$ profile must be fine-grained within this dimension. In practice, condensation of 4–10 nm silica layers onto nanoparticles is possible [15], thus the goal of achieving Hermite scatterers through the visible light spectrum is plausible. In acoustics with much longer wavelengths the scale increases proportionally.

4. Conclusion

Spherically symmetric scatterers with varying acoustic or dielectric properties can now be constructed in layers as concentric thin shells. This motivates a re-examination of specific inhomogeneity functions that can be used to create unique scattering signatures. In particular, material properties prescribed to modified Hermite functions of odd orders m will produce long wavelength backscatter amplitudes proportional to $k^{(m+1)}$. Realizations of these inhomogeneities offer the capability to modify the color of backscattered light from different classes of Hermite scatterers and create unique identification schemes based on detection of the specific power laws. This is particularly relevant in the use of optical tracer particles [21] and ultrasound contrast agents [22] used in industrial and medical applications.

Acknowledgements

We are indebted to Professor Robert Waag for his illuminating explanations of scattering, and to Professor Andrew Berger for his insightful suggestions. This work was supported by the Hajim School of Engineering and Applied Sciences at the University of Rochester.

References

[1] M. Abramowitz, I.A. Stegun, Handbook of Mathematical Functions with Formulas, Graphs, and Mathematical Tables, U.S. Govt. Print. Off., Washington, 1964.
[2] F. Baletto, C. Mottet, R. Ferrando, Growth of three-shell onionlike bimetallic nanoparticles, Phys. Rev. Lett. 90 (2003) 135504.
[3] M. Born, E. Wolf, Principles of Optics: Electromagnetic Theory of Propagation, Interference and Diffraction of Light, Pergamon Press, London, 1980, Chapter 13.
[4] J.A. Campbell, R.C. Waag, Ultrasonic scattering properties of three random media with implications for tissue characterization, J. Acoust. Soc. Am. 75 (1984) 1879–1886.
[5] P. Debye, A.M. Bueche, Scattering by an inhomogeneous solid, J. Appl. Phys. 20 (1949) 518–525.
[6] A. Erdélyi, H. Bateman, Tables of Integral Transforms, vol. 1, McGraw–Hill, New York, 1954.
[7] J.C.M. Garnett, Colours in metal glasses and in metallic films, Philos. Trans. R. Soc. Lond. A 203 (1904) 385–420.
[8] M.F. Insana, R.F. Wagner, D.G. Brown, T.J. Hall, Describing small-scale structure in random media using pulse-echo ultrasound, J. Acoust. Soc. Am. 87 (1990) 179–192.
[9] A. Ishimaru, Wave Propagation and Scattering in Random Media, Academic Press, New York, 1978.
[10] G. Mie, Beiträge zur Optik trüber Medien, speziell kolloidaler Metallösungen, Ann. Phys. 330 (1908) 377–445.
[11] P.M.C. Morse, K.U. Ingard, Theoretical Acoustics, Princeton University Press, Princeton, 1968.
[12] K.J. Parker, The H-Scan format for classification of ultrasound scattering, OMICS J. Radiol. 5 (2016) 1000236.
[13] K.J. Parker, Scattering and reflection identification in H-scan images, Phys. Med. Biol. 61 (2016) L20-8.
[14] A.D. Poularikas, Transforms and Applications Handbook, CRC Press, Boca Raton, FL, 2010.
[15] E. Prodan, C. Radloff, N.J. Halas, P. Nordlander, A hybridization model for the plasmon response of complex nanostructures, Science 302 (2003) 419–422.
[16] L. Rayleigh, XXXVII. On the passage of waves through apertures in plane screens, and allied problems, Philos. Mag. Ser. 5 43 (1897) 259–272.
[17] L. Rayleigh, On the scattering of light by spherical shells, and by complete spheres of periodic structure, when the refractivity is small, Proc. R. Soc. Lond. A-Cont. 94 (1918) 296–300.
[18] J.W. Strutt, Investigation of the disturbance produced by a spherical obstacle on the waves of sound, Proc. Lond. Math. Soc. s1-4 (1871) 253–283.
[19] R.C. Waag, D. Dalecki, P.E. Christopher, Spectral power determinations of compressibility and density variations in model media and calf liver using ultrasound, J. Acoust. Soc. Am. 85 (1989) 423–431.
[20] R.C. Waag, D. Dalecki, W.A. Smith, Estimates of wave front distortion from measurements of scattering by model random media and calf liver, J. Acoust. Soc. Am. 85 (1989) 406–415.
[21] C. Kähler, B. Sammler, J. Kompenhans, Generation and control of tracer particles for optical flow investigations in air, Exp. Fluids 33 (2002) 736–742.
[22] B.B. Goldberg, J.S. Raichlen, F. Forsberg, Ultrasound Contrast Agents: Basic Principles and Clinical Applications, Martin Dunitz, London, 2001.